Photogating of ionic currents across lipid bilayers

Hydrophobic ion conductance by an ion chain mechanism

Charles M. Drain and David C. Mauzerall
The Rockefeller University, New York, New York 10021 USA

ABSTRACT The photogating of hydrophobic ion currents across the lipid bilayer membrane allows the direct study of their kinetics by symmetrically forming charge within the membrane and across each interface, rather than across the membrane. We find that the photoinduced conductance continues to increase beyond the region where the tetraphenylboride charge density in the membrane exceeds the estimated porphyrin cation density. This photoconductance is proportional to the tetraphenylboride charge density raised to the second to third power. The risetime of the photogating effect increases with increasing concentration of tetraphenyl boride. The porphyrin cation mobility is increased when the tetraphenylboride anion is present, and low concentrations of tetraphenylphosphonium cation increase the dark conductivity while inhibiting the photoconductivity. The activation energy for both the porphyrin and phosphonium cation induced conductance is more positive than that of the tetraphenylboride conductance. From these results we conclude that in addition to some cancellation of space charge within the membrane, the mechanism of increased conductance involves the transport of these hydrophobic anions via an alternating anion-cation chain, analogous to the Grotthuss mechanism for excess proton conduction in water. This ion chain conductance can be viewed as an evolutionary prototype of an ion channel across the membrane. It also underscores the importance of the counter ion in the transport of large ions such as peptides across the lipid bilayer.

GLOSSARY

A_m	membrane area (8×10^{11} nm^2)
β	hydrophobic ion partion coefficient (nm)
d_m	membrane thickness (8 nm)
G_{dk}	conductance in the dark, (S)
G_{ph}	conductance in the light, (S)
ΔG	Photoconductance, $G_{ph} - G_{dk}$ (S)
I_{dk}	current in the dark, (A)
I_{ph}	current in the light, (A)
$\mu_{TPhB^-/BLM}$	mobility of $TPhB^-$ in membrane (12 nm^2 s^{-1} V^{-1})
$\mu_{TPhB^-/water}$	mobility of $TPhB^-$ in water (2×10^{10} nm^2 s^{-1} V^{-1})
q	electronic charge (1.6×10^{-19} coulomb)
ρ_{P+}	charge density of the porphyrin cation (nm^{-2})
ρ_{TPhB^-}	charge density of the boride anion (nm^{-2})
V	potential (V)

INTRODUCTION

The mechanism by which ions cross cell membranes is a fundamental question in many areas of biology since these currents are essential for all living cells (Hille, 1984; Honig et al., 1986). These ionic currents have been examined by monitoring the voltage relaxations after an applied charge step or by monitoring the current relaxations after an applied voltage step across bilayer lipid membranes containing ion channels, ion carriers, or hydrophobic ions (Andersen et al., 1978; Lauger et al., 1981; Bender, 1988). These techniques have been very useful but are limited by the capacitative transient of the membrane and by ambiguity of interpretation of the data (Pickar and Hobbs, 1982). We have shown that the conductance of hydrophobic ions can be gated by the photogeneration of charge inside the membrane (Drain et al., 1989; Mauzerall and Drain, 1992). The photogating technique avoids the problems associated with the charge and voltage pulse techniques by minimizing the membrane capacitative transients. Since photocharging the membrane can occur on the nanosecond time scale (Woodle et al., 1987), the fast kinetics of ion transport can in principle be directly observed. We now apply the photogating technique to a study of the kinetics of hydrophobic ion currents and propose a mechanism for the conductances. Based on several different kinds of data, it is concluded that the direct electrostatic effects account for the rapid, small changes of conductivity but the slow, large changes require an ion-chain or Grotthuss mechanism. This latter may be a prototype of an ion channel. The mechanism suggests a role for large counter ions in the transport of charged proteins across the lipid bilayer.

Address correspondence to Dr. David C. Mauzerall, The Rockefeller University, 1230 York Avenue, New York, NY 10021 USA.

METHODS

A complete description of the materials and methods has been reported (Mauzerall and Drain, 1992). Typically a ±40-mV square wave of variable duration is applied across a membrane composed of diphytanoylphosphatidylcholine/decane (3% wt/vol; Avanti Polar Lipids, Inc., Birmingham, AL) containing 3.6 mM magnesiumoctaethylporphyrin (MgOEP). The 1-μs flash lamp pumped dye laser containing rhodamine-6G is triggered ~1 s after the membrane capacitative transient after a voltage change of a given sign. The time constant of the operational amplifier is typically set at 100 μs, and the data are collected (up to 16 traces) by a transient recorder (model 194; Keithley Instruments, Cleveland, OH) and averaged on a computer (model 318; Hewlett-Packard, Palo Alto, CA). The hydrophobic ion and aqueous accepter are added symmetrically across the membrane from stock ethanol-water (50% vol/vol) solutions such that the final concentration of ethanol in the bathing solutions never exceeded 1% by volume. Anthraquinone-2-sulfonate(−1) (AQS^-) is used with tetraphenylboride anion($TPhB^-$) and methylviologen(+2) is used with tetraphenylphosphonium cation ($TPhP^+$) to avoid complex formation between the

0006-3495/92/12/1556/08 $2.00

hydrophobic ion and the electron acceptor. The buffer solutions consist of 100 mM NaCl and 10 mM *N*-2-hydroxyethylpiperazine-*N'*-2-ethane sulfonic acid (Hepes), adjusted to pH 7.2. The continuous white light experiments used a 300-W tungsten/halogen projector lamp resulting in 25 mW cm^{-2} s^{-1} at the membrane. Although both positive and negative voltages yield similar results, as shown in Fig. 1, for clarity only the absolute values of the conductance, current, and voltage data are shown in the figures. Activation energies are determined by repeating the room temperature laser pulse experiments at temperatures between 5 and 40°C in a water jacketed cell.

RESULTS AND DISCUSSION

The relevant conclusions of the electrostatic model (Mauzerall and Drain, 1992) are (*a*) the electrostatic calculations indicate that the large photogating effect at high $TPhB^-$ concentrations cannot be entirely due to cancellation of the $TPhB^-$ space charge by the porphyrin cations; (*b*) the dark conductance G_{dk} may be near the diffusion limit at $TPhB^-$ concentrations below 0.7 μM,

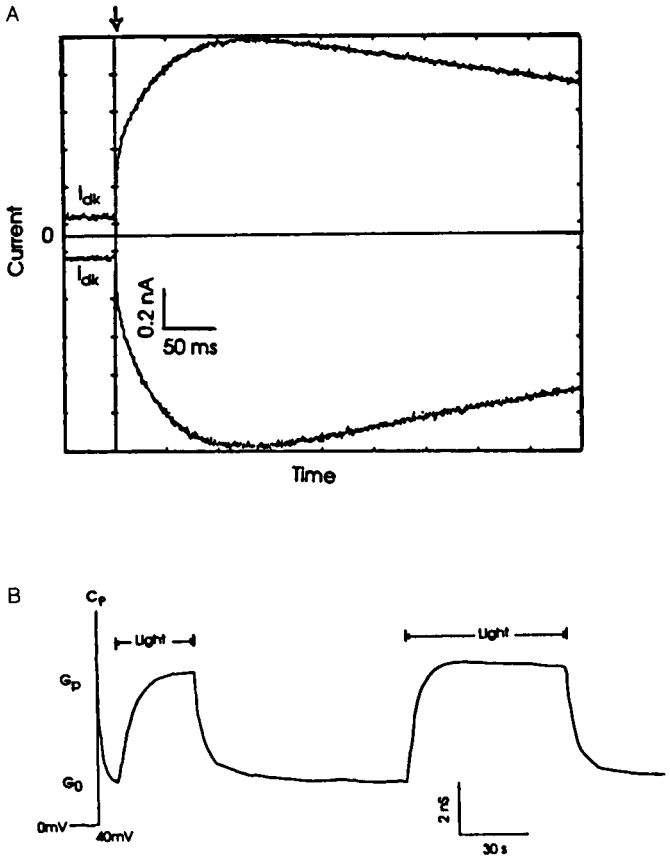

FIGURE 1 (*A*) The ionic current of 6 μM $TPhB^-$ increases 10-fold after a 1-μs saturating pulse of 596-nm light on the diphytanoylphosphatidylcholine/decane membrane containing MgOEP with 0.1 M NaCl, 10 mM Hepes at pH 7.1, and 0.1 mM AQS^- on each side of the membrane. The top and bottom traces are recorded with + and −40 mV, respectively. The instrumental time constant is 100 μs, the light pulses are indicated by the arrow, and the baseline current by I_{dk}. (*B*) The dark and photo current of 2.67 μM $TPhB^-$ upon continuous illumination with white light. The capacitative transient on turning on the applied voltage is labeled *Cp*.

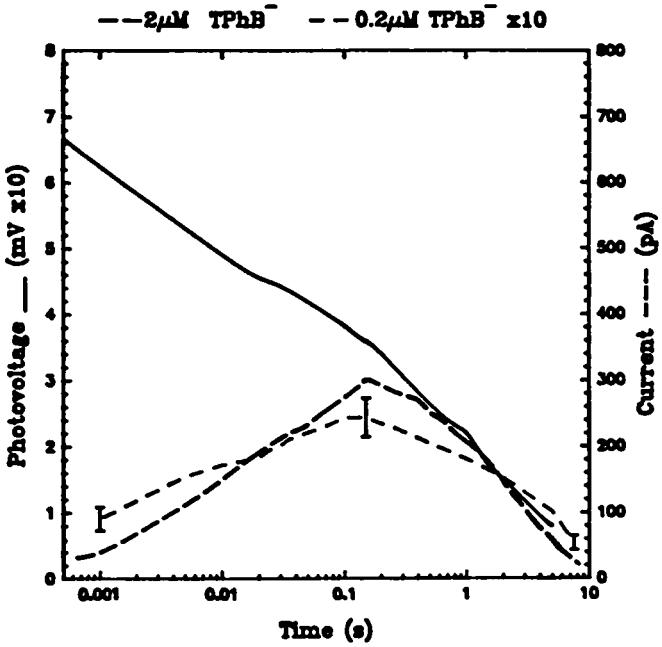

FIGURE 2 The photovoltage and the photo conductance signals are plotted versus log time. The photovoltage, obtained when the electron accepter is on only one side of the membrane and there is no applied voltage, is represented by the solid line. The photovoltage is multiplied by 10 to scale it to the photogating signal. The photo conductance signal, obtained when the acceptor is symmetric and there is an applied voltage of +40 mV, is represented by the dashed lines. The long dashes represent the current of 2 μM $TPhB^-$ and the short dashes represent the current from 0.2 μM $TPhB^-$ ×10. The instrumental time constants are 100 μs for the 2 μM data and 1 ms for the 0.2 μM data.

and the maximal conductance after a light pulse, G_{ph}, is near the linear nonspace charge limited conductance at all concentrations; and (*c*) the ionic strength of the bathing solutions predominantly effects the binding constant (β) of these ions and not their conductance.

At high concentrations of $TPhB^-$, where G_{dk} is saturated due to space charge inside the bilayer (Mauzerall and Drain, 1992), G_{ph} increases up to 15-fold on photoformation of MgOEP cation. Fig. 1 *A* shows a 10-fold increase in $TPhB^-$ current on photocharging the membrane with a 1-μs laser pulse at positive and negative applied voltages. The number of charges gated is up to 25 times the estimated amount of porphyrin cation formed. When the photogating system is irradiated with continuous white light, the signal, $\Delta G/G_{dk}$ is 300% (Fig. 1 *B*), which is 75% of the maximal pulsed photosignal under the same conditions. It decreases by only 10–15% over the next 4 min when the bathing solutions are stirred, and this process is repeatable for the lifetime of the membrane. These results and the chemical oxidation experiments (Drain et al., 1989) show that an actual increase of conductance occurs and not just a transient membrane depolarization.

Fig. 2 shows the photo conductance and photovoltage signals (the later from an asymmetric acceptor experi-

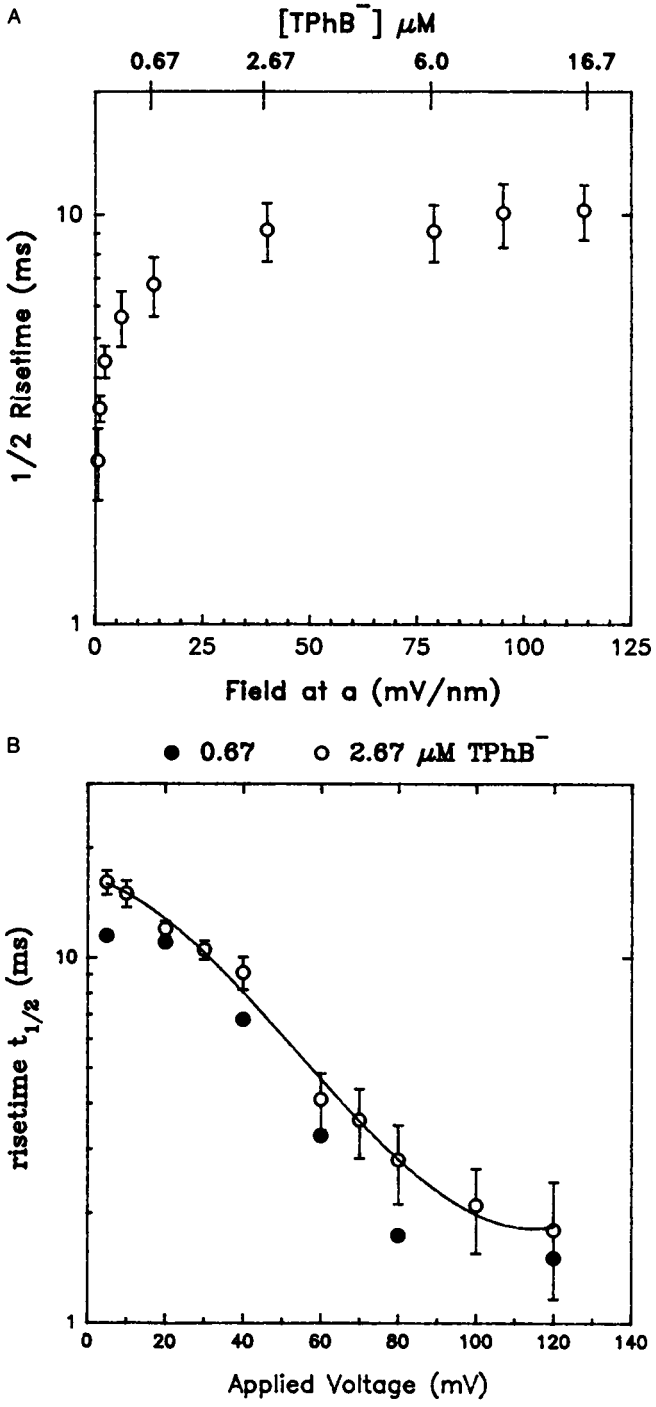

FIGURE 3 (*A*) The half rise time, $t_{1/2}$, of G_{ph} versus electric field at the lattice (*a*) of $TPhB^-$. The field is calculated with the exponential-core model described in the companion article (Mauzerall and Drain, 1992). The applied voltage is ±40 mV. (*B*) The half rise time, $t_{1/2}$, versus applied voltage at two $TPhB^-$ concentrations. The closed circles represent the 0.67 μM and the open circles represent the 2.67 μM $TPhB^-$ data. The line fitting the data at the higher concentration is arbitrary. Each voltage experiment is performed on only one membrane for the entire range of voltages, and the 2.67 μM data is the average of three membranes.

ment with no applied voltage) on a log-time scale so the entire time course of these signals can be compared. The slopes of the photovoltage and the G_{ph} decays are similar. There is always a fast component of the photoconductance signal (risetime <100 μs) that is not resolvable in the present experiments. The approximate linearity of the signals as a function of log time characterize distributed kinetics (Liu and Mauzerall, 1985). Removing dioxygen from the system with a glucose/glucose oxidase/catalase protocol (Ilani et al., 1985) has only a small <5% effect on the amplitude or decay of these photoinduced currents. The decay time is found to be only slightly dependent on the applied voltage, <25% from 40 to 100 mV, and on lipophilic ion concentration, decreasing from 3 to 2 s at 0.067 to 3.33 μM $TPhB^-$, all at ±40 mV.

The binding of $TPhB^-$ to the membrane decreases with increasing space charge (Mauzerall and Drain, 1992). The risetime of the photo conductance *increases* with concentration of $TPhB^-$ and thus with space charge (Fig. 3 *A*). The data are plotted versus the estimated field at the position of the $TPhB^-$ lattice calculated using the exponential-core electrostatic model (Mauzerall and Drain, 1992). The field for one-half change in risetime, ~10 mV/nm, will be related to the ion chain mechanism (see below). The risetime of the photo conductance decreases with the applied voltage (Fig. 3 *B*). The voltage for a half change of the kinetics is ~40 mV and decreases slightly at lower $TPhB^-$ concentrations.

Both G_{dk} and G_{ph} are approximately independent of applied voltage at a high concentration (3.33 μM), of $TPhB^-$ (Fig. 4). The more sensitive plot of $\Delta G/G_{dk}$ indicates a lag in the conductance with applied voltage. Small asymmetries in the input voltage arising from both the calomel electrodes and the voltage source, which have been approximately corrected, may contribute to the total error.

Mechanism

If we define $G_{dk} = q\mu_{TPhB^-}\rho_{TPhB^-}A_m/d_m^2$, where A_m is the area of the membrane, d_m is the thickness of the membrane, q is charge, ρ_{TPhB^-} is the charge density of $TPhB^-$, then the simple assumption that the bulk mobility (μ_{TPhB^-}) is constant implies that the conductance is determined by the charge density alone. This assumption, along with the electrostatic calculations of the normalized potential, allows one to fit the G_{dk} saturation data with reasonable values of ρ_{TPhB^-}:

$$\rho_{TPhB^-} = 0.602C\beta \exp(-qV_{\rho TPhB^-}), \quad (1)$$

(Mauzerall and Drain, 1992). In fact, the calculated value of $\rho_{TPhB^-} = 0.07\ nm^{-2}$ at $C = 1$ μM $TPhB^-$ is the same as that found by Andersen et al. (1975, 1978) based on capacitative transient measurements. However, the photo conductance increases transiently up to, or somewhat greater than, that of the linear, nonspace

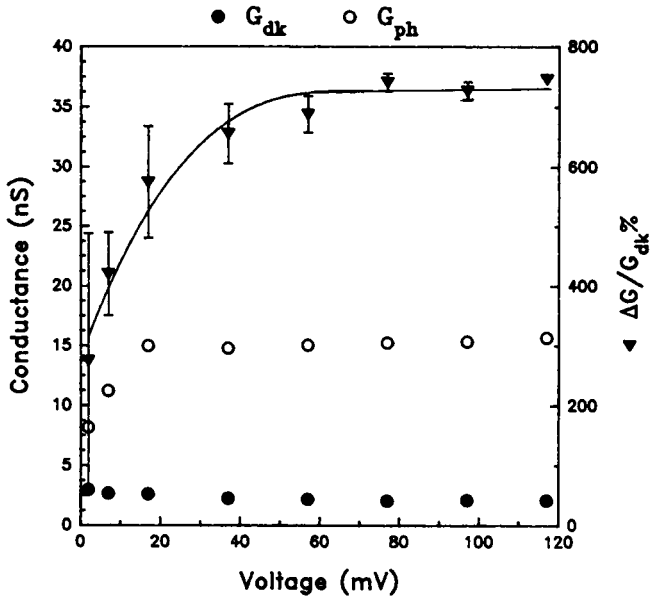

FIGURE 4 Voltage dependence of the photogating effect at 3.33 μM $TPhB^-$, 0.1 M NaCl, and positive voltages only. G_{dk}, *filled circles*; G_{ph}, *open circles*; and $\Delta G/G_{dk}$, *open triangles*. The line through the $\Delta G/G_{dk}$ data is arbitrary. The conductance plotted is the observed current divided by the applied voltage corrected for electrode asymmetry.

charge limited value, suggesting that the space charge due to the $TPhB^-$ lattice has been cancelled by that of the porphyrin cation lattice (Fig. 2 in Mauzerall and Drain, 1992). The largest ρ_{TPhB^-} estimated is ~0.2 nm^{-2}, whereas our estimate of ρ_{P+} is ~0.008 (Drain et al., 1989; Mauzerall and Drain, 1992). The electrostatic calculations show that the photoformation of the $MgOEP^+$ lattice at reasonable positions in the bilayer is unable to cancel the space charge entirely, and thus a purely electrostatic mechanism cannot account for the large increase in the photogating conductance.

This state of affairs can be bypassed in two ways. One is a specific ion-chain mechanism discussed below. The second possibility is to allow the mobility to decrease with space charge, which would increase the dependence of the G_{ph} on V and thus on ρ_{TPhB^-}. The result is a fit with a smaller ρ_{TPhB^-}, one more compatible with the estimated ρ_{P+}. However, even if the mobility is made as equally dependent as β (Eq. 1) on the internal potential, the fit to the dark conductivity requires ρ_{TPhB^-} to be smaller by only a factor of two. To reduce ρ_{TPhB^-} by a large factor would require the mobility to be determined by the larger potential at the center of the membrane. Anderson et al. (1975, 1978) claim that the mobility of $TPhB^-$ is rapid in the membrane, with the slow step at the interface. However, their analysis was for the linear region of boride conductance, <1 μM $TPhB^-$. Our observation of a slowing rise time of the photo conductance with increasing $TPhB^-$ concentration and internal field (Fig. 3 *A*), supports the view that the ion movement is slowed by the space charge and that the space charge is not entirely cancelled by $MgOEP^+$. This view is further supported by the limiting photogating effect of ~30% at low $TPhB^-$ concentrations, i.e., in the linear region (Fig. 2 of Mauzerall and Drain, 1992). Here, ρ_{P+} may exceed ρ_{TPhB^-}, reversing the sign of the space charge. Maximizing ρ_{P+} by assuming the conductance increase is only caused by a change in ρ_{TPhB^-} via Eq. 1 implies a ΔV of +8 mV corresponding to a ρ_{P+} of only ~0.005 nm^{-2} in agreement with our estimate from the photovoltage, 0.008 nm^{-2} (Mauzerall and Drain, 1992). Moreover, this limited increase in photo conductance occurs on a fast time scale (<1 ms) as expected for the space charge cancellation by the photo formed porphyrin cations. This is in striking contrast to the slower, space charge dependent rise time of the large (>100%) increase in the photo conductance in the space charge limited region (Fig. 3 *A*). The fraction of very fast photo conductance also decreases with increasing. $TPhB^-$ (Fig. 2). Thus, we conclude that the large increase in G_{ph} is caused by a different mechanism of ion transport than that active at low concentration of $TPhB^-$. When $\Delta G/G_{dk} = 1$, ρ_{P+} is estimated to cancel only 10% of the $TPhB^-$ space charge. Thus, at constant light energies, $MgOEP^+$ formation would be expected to cancel a smaller and smaller fraction of the $TPhB^-$ space charge as ρ_{TPhB^-} increases, such that at $\Delta G/G_{dk} = 10$, only ~3% of the space charge would be cancelled by ion pair formation. Yet the photo conductance increases, further supporting the view that space charge cancellation is not entirely responsible for the large photoeffect.

The ion chain mechanism is composed of two to three cation-anion pairs that align, and, by transfer of a $TPhB^-$ at each interface, an ion hops across the membrane (Fig. 5). It is not unreasonable to expect that $MgOEP^+$:$TPhB^-$ ion pairs will form. Both anion and cation are positioned in the ester region of the bilayer. The rate of the formation of $TPhB^-$:$MgOEP^+$ ion pairs depends on the $\rho_\pm$ of these ions. For example, if ρ_{TPhB^-} is 0.05 nm^{-2}, the $MgOEP^+$ is at the center of the lipophilic ion lattice, and if the translational diffusion constant for these ions is similar to the planar diffusion of the lipids, 4×10^6 nm^2 s^{-1} (Javin and Vay, 1989), then the average time for the formation of the ion pair is ~2 μs. Moreover, the electrostatic attraction will shorten this time. Similar rates are expected for the formation of the $TPhB^-$:$MgOEP^+$:$TPhB^-$ aggregate. The time for the alignment of $TPhB^-$:$MgOEP^+$ pairs on one side of the bilayer with those on the other side would be <50 μs except at very low ρ_{P+}. Thus, the formation of the ion chain is not rate limiting.

Since the $TPhB^-$ and $MgOEP^+$ are present on each side of the membrane, the ion pairs will form on each side (Fig. 5, step *A*). Once the $MgOEP^+$:$TPhB^-$ pair is formed, it is a dipole and, in the absence of internal fields, will orient according to the applied voltage such that the ion pair on one side of the membrane will have the same orientation as the other (Fig. 5, step *B*). The

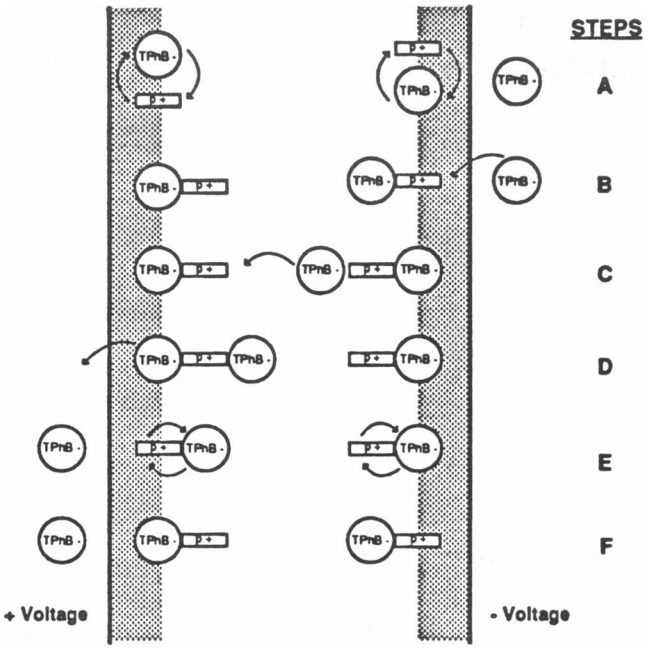

FIGURE 5 Schematic of the ion-chain mechanism for the photogating of ionic currents across the lipid bilayer. The width of the membrane and the size of the $MgOEP^+$ (*rectangles*), and the $TPhB^-$ (*circles*), are to scale. The lipid head groups are represented by the shaded areas. Individual ions are represented as rectangles or circles, whereas ion pairs and aggregates are shown as connecting circles and rectangles. The individual steps (*A–F*), are discussed in the text.

rate of this orientation will depend on the applied voltage. Now the ionic dipole has the correct orientation to accept a boride ion from the bulk or one already bound to the membrane. This ion aggregate can donate the inner $TPhB^-$ to the ion dipole on the other side of the membrane (Fig. 5, step *C*). Once the $TPhB^-$:$MgOEP^+$:$TPhB^-$ ion is formed on the other side of the membrane it "dissociates" a $TPhB^-$ ion into the aqueous phase (Fig. 5, step *D*). The resulting ion dipoles then reorient in the applied field (Fig. 5, step *E*). Once the ion pair is reoriented it is ready to repeat the sequence (Fig. 5, step *F*). We refer to the mechanism where the $TPhB^-$ is transferred from one ion pair to the other as the ion chain mechanism and it is similar to the Grotthuss mechanism for the excess conductivity of H^+ and OH^- in water (see Moore, 1962). Essentially, the electrostatic barrier to movement is smaller for the dipole than for an individual ion. For the case of equal-sized spheres, the Born charging energy of the ion pair is one-half that of the individual ions. For the case of excess $TPhB^-$ and weak ion binding, the conductance is expected to be proportional to $\rho_{P^+}(\rho_{TPhB^-})^{n+1}$, where n is the number of ion pairs participating in the ion chain. The light saturation curve for $\Delta G/G$ has a similar slope as that of the photovoltage and indicates the photogating is proportional to the amount of porphyrin cation formed in the membrane (Fig. 6). Plots of log ΔG versus log ρ_{TPhB^-} at three ionic strengths have slopes of 2.7 ± 0.1 in the rapidly increasing range (Fig. 7), suggesting that three $TPhB^-$ ions are involved in the crossing step.

The ion chain mechanism predicts that the mobility of the porphyrin cation will be increased along with that of the boride anion. The photovoltage is ~30% less in magnitude and decays ~40% faster (Table 1) when a donor such as ascorbate is placed on the opposite side of the membrane from the electron acceptor in the presence of $TPhB^-$. More recent experiments with substituted tetraphenylborides show much larger effects (Sun, K., and D. C. Mauzerall, unpublished data). Previous experiments have always shown no effect of donors on the side of the membrane opposite that of the acceptor (Hong and Mauzerall, 1976; Woodle and Mauzerall, 1986). Both effects are smaller with ferrocyanide (Table 1). When $MgOEP^+$ is formed on only one side of the membrane and that side is charged negatively, the photoconductance is ~40% of that when $MgOEP^+$ is formed on both sides. If the porphyrin cation did not move, the remaining space charge on the nonporphyrin side would effectively block the photogating effect. If the porphyrin cation does move, the halving of the effect is expected because of the 50% decrease in the cation. This experi-

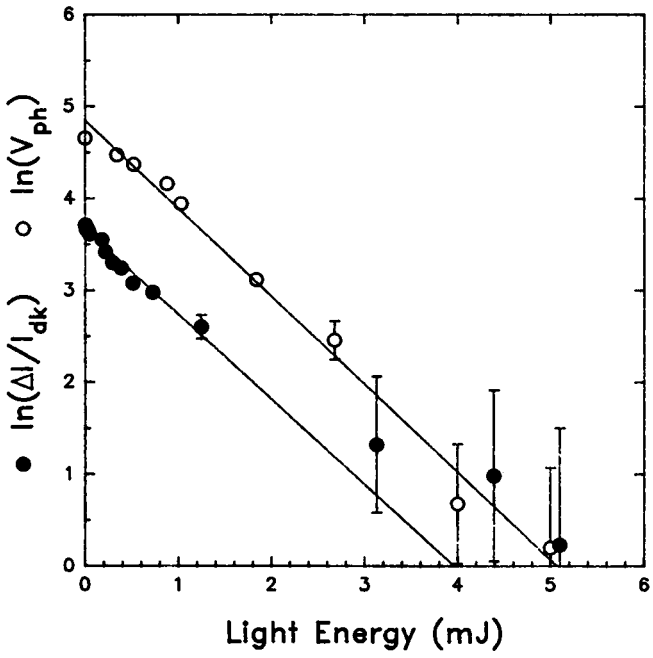

FIGURE 6 The open circles are a plot of the saturation of the photovoltage and the filled circles are a plot of the saturation of $\Delta I/I_{dk}$, ($=\Delta G/G_{dk}$) with light energy; 0.67 μM $TPhB^-$ at ±40 mV. The linear least-squares fit of the $\Delta I/I_{dk}$ data does not include the two points at the highest light energy, and the photovoltage data has been scaled by 10. For the photo current saturation plot, the natural log of the difference between the $\Delta I/I_{dk}$ in saturating light and $\Delta I/I_{dk}$ at lower light energies is plotted versus light energy. For the photovoltage saturation plot, the natural log of the difference between the photovoltage in saturating light and that at lower light energies is plotted versus light energy.

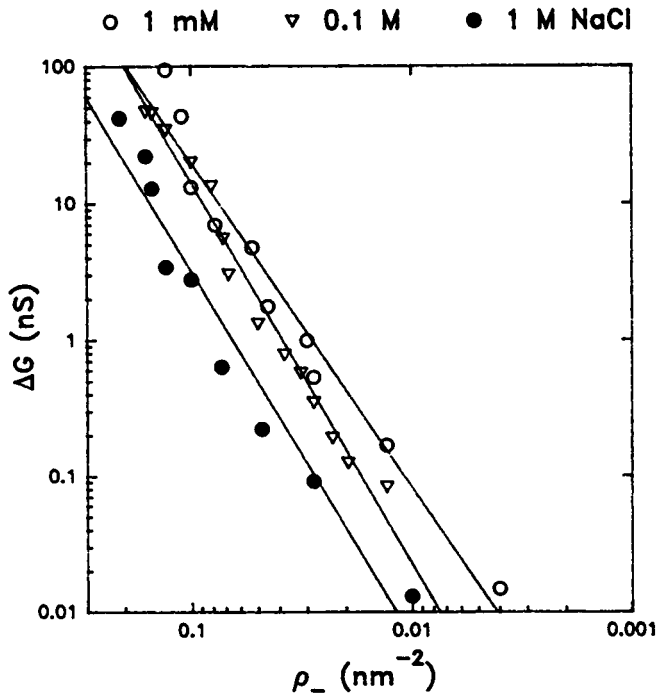

FIGURE 7 The linear region of a log-log plot of ΔG versus ρ_{TPhB^-} at ionic strengths of 1 mM, 0.1 M, and 1 M. The slopes are 2.7 ± 0.1, indicating that about three $TPhB^-$ are involved in the photogating mechanism. The data are taken from Fig. 2 in companion article (Mauzerall and Drain, 1992).

ment also displays an asymmetry in the magnitude of the photosignal with sign of the applied voltage. When a positive voltage is applied to the side of the membrane containing the $MgOEP^+$, the photosignal is only 17% of the symmetrical case compared with 40% when a negative voltage is applied (Table 1). This may be caused by some polarization by the applied voltage. The increased

TABLE 1 **Effects of asymmetric acceptor and donors**

Experiment	$\Delta G/G_{dk}$	Photovoltage	Photovoltage decay $t_{1/2}$
	%	*mV*	*ms*
Photogating: 1.67 μM $TPhB^-$	300		
AQS^{-1} one side, −40 mV	121		
AQS^{-1} one side, +40 mV	50		
Photovoltage: 0.1 mM AQS^{-1} on one side		2.0	128
3 μM $TPhB^-$		1.9	120
3 μM $TPhB^-$, ascorbate opposite side		1.4	74
3 μM $TPhB^-$, ferrocyanide opposite side		1.6	93

Summary of the asymmetric photogating and donor/acceptor experiments. The photogating experiments have equivalent amounts of $TPhB^-$ on each side of the membrane and 0.1 mM AQS^{-1} on only one side of the membrane. The resulting photovoltage, ~2 mV, is only ~5% of the 40-mV applied voltage, thus no correction for its effect is made. For the donor/acceptor experiment, where there is no applied voltage, ferrocyanide (1 mM) or ascorbate (1 mM) donors are placed on the opposite side of the membrane as the AQS^-.

$TPhB^-$ on the positive side may slow the redistribution time and thus lose P^+ to its decay (Fig. 2).

The ion chain mechanism predicts that any large cation will increase the mobility of the hydrophobic anion. In fact, G_{dk} of $TPhB^-$ increases on adding low concentrations of $TPhP^+$, whereas G_{ph} simultaneously decreases (Fig. 8). If the photogating mechanism only concerned the effect of space charge, then the conductance would be expected to continue to increase with increasing concentrations of $TPhP^+$ instead of saturating and there would be no reason for inhibition of the photo-effect. The conduction with $TPhP^+$ saturates at approximately two-thirds of that with the porphyrin cation. This in itself may support the ion chain mechanism because of the different size and symmetry of the $MgOEP^+$ and $TPhP^+$ cations. The disk shaped $MgOEP^+$ "fits" into the lipid bilayer much more readily than the tetrahedrally shaped tetraphenylboride ions. The low concentration of $TPhP^+$ required, ~100 less than that needed for equal conductance in the absence of $TPhB^-$, is a manifestation of Eq. 1, with a positive sign in the exponential. The higher concentration of $TPhB^-$ required to saturate G_{ph} (5 μM) compared with that required to increase G_{dk} (2 μM) (Fig. 8), may be a reflection of the increase of G_{dk}. Similar effects are seen at a nonsaturating concentration of $TPhB^-$ (Fig. 8). The enhanced conductance of mixtures of $TPhB^-$ and $TPhP^+$ has been observed in submitochondrial particles (Grinius et al., 1970).

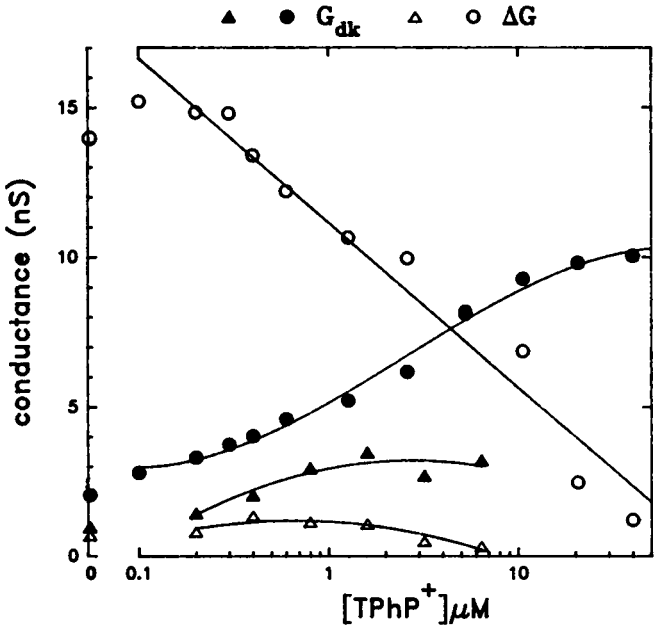

FIGURE 8 The increase in G_{dk} (*closed circles*), and decrease in ΔG (*open circles*), of 3 μM $TPhB^-$ versus the concentration of $TPhP^+$ in the bathing solutions. The closed and open triangles represent G_{dk} and ΔG of 0.4 μM $TPhB^-$ versus $TPhP^+$ concentration. A ±40 mV voltage is applied across the membrane.

The ion-chain mechanism makes definite predictions concerning the activation energy of the conductance. The applied electric field favors the correct alignment of the ion pairs for $TPhB^-$ hopping down the field. However, the presence of other fields, in particular those of the $TPhB^-$ lattice itself, will add an activation energy since the $TPhB^-$ field must be contrary to the alignment of the ion pair in one or the other half of the membrane. This is because the sum of the internal fields is equal to zero. Thus, at least one of the ion pairs in the chain (Fig. 5), will be energetically unfavored by the internal field. Since the plane of the porphyrin remains perpendicular to the plane of the membrane because of its alignment with the lipids (Ishikawa and Kunitake, 1991), the dipole moment of the $MgOEP^+$:$TPhB^-$ pair is one full charge separated by 1 nm. Our estimate of the internal field from the $TPhB^-$ lattice at half saturating concentrations is ~10 mV/nm (Fig. 3 *A*). The orientation energy will be twice the dipole moment times the field or ~1 kT. This may explain the increasing rise time with increasing $TPhB^-$ concentration: it should track this field, as observed in Fig. 3 *A*. If the applied voltage is "dropped" across only one-half of the bilayer thickness, then the possible lag in the photoconductivity with voltage (Fig. 4), could also be explained. At applied voltages <10 mV, the applied field would be less than the internal field. Possibly the many body effects of the space charge translate these small equilibrium electrostatic energies into the observed slow rates. The definite saturation of conductance with voltage is not expected. Possibly at high $\rho_\pm$, the $TPhB^-$ may directly exchange sites near P^+, bypassing the need for dipole rotation. The dynamics of ion movement in the space charged region are rather complex even in the absence of counter charged ions (De Levie, 1978), and we must leave their description to the future.

The activation energy of the conductances was measured at 3.3 μM $TPhB^-$ over the temperature range of 6 to 30°C. The gel transition for diphytanoyl phosphocholine is well below 0°C (Avanti Polar Lipids, Inc., private communication). The activation energy for G_{ph} is 14 ± 2 kcal mol^{-1} and for G_{dk} is 5 ± 2 kcal mol^{-1}. The striking difference between the energies of the dark conductance and the photoconductance is a certain sign of differing mechanisms. Note that the reverse effect, a smaller activation energy of the photoconduction, would be expected if the porphyrin cation cancelled the boride space charge that causes the conductance to saturate by adding an electrostatic barrier. Since the dark current may be partially limited by depletion in the water layer, the smaller activation energy of the viscosity of water, ~4 kcal mol^{-1}, may contribute to its small measured activation energy. The activation energy for conductance is composed of a binding enthalpy for β and an activation energy for $\mu_{TPhB^-/BLM}$, essentially that of viscosity. A direct calorimetric determination of ΔH for β gives −9 kcal mol^{-1} (Schere and Seelig, 1989; Seelig and Ganz, 1991) and the temperature dependence of charge pulse transient gives −7 kcal mol^{-1} (Benz, 1988), but determinations via indirect measures of β versus temperature (quoted by Flewelling and Hubble, 1986) give -2 ± 2 kcal mol^{-1}. The activation energy of transient conductance determined by Benz (1988) is 10 kcal mol^{-1} and that quoted by Flewelling and Hubble (1986) is 14 kcal mol^{-1}, in agreement with that of our photoconductance and not with that of our dark conductance. If ΔH of β is −8 kcal mol^{-1}, the activation energy of $\mu_{TPhB^-/BLM}$ in the dark is +13 kcal mol^{-1}. By comparison, the activation energy for diffusion of pyrene in egg lecithin is 7 kcal mol^{-1} (Vanderkooi and Callis, 1974) and for rotational diffusion of 12-(9-anthroyl) stearate in L-α-dipalmitoyl phosphocholine is 10 kcal mol^{-1} above the transition temperature (Vanderkooi et al., 1974). The somewhat larger value of $TPhB^-$ may be caused by electrostatic effects, e.g., Born energies, and the fact that ionic mobility measures strictly the perpendicular component of the anisotropic viscosity, whereas other measurements weight the lateral component. The ion chain mechanism will have viscosity dependent terms for the rotation of the ion pairs. Since at least two such independent reactions must be concerted in one ion chain, a larger activation energy, 15–20 kcal mol^{-1} is expected, as is observed. In agreement, the risetime kinetics also show a large activation energy of 13 ± 3 kcal mol^{-1} (data not shown). Finally, the activation energy of the $TPhB^-/TPhP^+$ conductivity measured at 3 μM $TPhB^-$ and 10 μM $TPhP^+$ is 10 ± 4 kcal mol^{-1}, a value consistent with the ion chain mechanism.

Charge sensitive ion conductor

The photogating system is an example of a working molecular electronic device that can be described as a photodriven field effect transistor (Carter, 1982; Hong, 1988), and we refer to it as a charge sensitive ion conductor (CSIC) (Drain and Mauzerall, 1990). The charge carriers are the hydrophobic ions, the source and drain are the ionic solutions at the two interfaces, the gate is composed of the self-formed space charge layer in the membrane, and it is controlled by the photochemically or chemically formed porphyrin cations. The switch of the CSIC can be turned on or off depending on the complementarity of the sign of the charge on the hydrophobic ions versus that on the photo or chemically formed ions. The present switch can be reversed by the anaerobic formation of the porphyrin anion.

Biological implications

The ion-chain mechanism of the photogating system can be thought of as a prototypical ion channel across the lipid bilayer. The photogating ion-chain mechanism is similar to the mechanism for the conductance of anions or cations through ion channels in that these ions are thought to hop from one charge or dipole to another

along the cavity of the channel. The lipophilic ions do not require the polar cavity because the Born charging energy of the ion pair is significantly less than that of the individual ion, and the alignment of two to three ion pairs may be sufficient to shuttle a lipophilic ion across the membrane. Both of these effects are related to the ~1-nm size of the ions. These considerations suggest the importance of the size of the counter ion in the transport of charged proteins or peptide segments across the lipid bilayer. Membrane transport proteins may contain amino acids of complementary charge and number to that of the protein being transported. Thus, relatively simple, self-assembling molecular structures form controllable transport systems that may have contributed to their biogenesis on the primitive earth.

We thank Dr. Kai Sun for help in measurements of the thermal activation parameters.

This research was supported by the National Institutes of Health grant GM-25693.

Received for publication 24 February 1992 and in final form 4 August 1992.

REFERENCES

Andersen, O. S., and M. Fuchs. 1975. Potential energy barriers to ion transport within lipid bilayers. *Biophys. J.* 15:795–830.

Andersen, O. S., S. Feldberg, H. Nakadomari, S. Levy, and S. McLaughlin. 1978. Electrostatic interactions among hydrophobic ions in lipid bilayer membranes. *Biophys. J.* 21:35–70.

Bender, C. J. 1988. Voltammetric studies of ion transfer across model biological membranes. *Chem. Soc. Rev.* 17:317–346.

Benz, R. 1988. Structural requirement for the rapid movement of charged molecules across membranes. Experiments with tetraphenyl borate analogues. *Biophys. J.* 54:25–33.

Carter, F. L. 1982. Molecular Electronic Devices. Marcel Dekker, New York. 400 pp.

DeLevie, R. 1978. Mathematical modelling of transport of lipid-soluble ions and ion-carrier complexes through lipid bilayer membranes. *In* Advances in Chemical Physics. I. Prigaogine and S. A. Rice, editors. J. Wiley & Sons, New York. 99–137.

Drain, C. M., and D. Mauzerall. 1990. An example of a working molecular charge sensitive ion conductor. *Bioelectrochem. Bioenerg.* 24:263–268.

Drain, C. M., B. Christensen, and D. Mauzerall. 1989. Photogating of ionic currents across the lipid bilayer. *Proc. Natl. Acad. Sci. USA.* 86:6959–6962.

Flewelling, R. F., and W. L. Hubbell. 1986. Hydrophobic ion interactions with membranes. *Biophys. J.* 49:531–540.

Grinius, E. L., A. A. Jasaitis, Y. P. Kadziauskas, E. A. Liberman, V. P. Skulachev, V. P. Topali, L. M. Tsofina, and M. A. Vladimirova. 1970. Conversion of biomembrane-produced energy into electric form: 1. Submitochondrial particles. *Biochim. Biophys. Acta.* 216:1–12.

Hille, B. 1984. Ion Channels of Excitable Membranes. Sinauer, Sunderland, MA. 426 pp.

Hong, F. 1988. Molecular Electronics: Biosensors and Biocomputers. Plenum Press, New York. 466 pp.

Hong, F., and D. Mauzerall. 1976. Tunable voltage clamp method: application to photoelectric effect in pigmented bilayer lipid membranes. *J. Electrochem. Soc.* 123:1317–1324.

Honig, B. H., W. L. Hubbell, and R. F. Flewelling. 1986. Electrostatic interactions in membranes and proteins. *Annu. Rev. Biophys. Biophys. Chem.* 15:163–193.

Ilani, A., T. M. Liu, and D. Mauzerall. 1985. The effect of oxygen on the amplitude of photodriven electron transfer across the lipid bilayer-water interface. *Biophys. J.* 47:679–684.

Ishikawa, Y., and T. Kunitake. 1991. Design of spatial disposition of anionic porphyrin in matrices of ammonium bilayer membranes. *J. Am. Chem. Soc.* 113:621–630.

Javin, T. M., and W. L. C. Vay. 1989. Rotational and translational diffusion in membranes measured by fluorescence and phosphorescence methods. *Methods Enzymol.* 172:471–513.

Lauger, P., R. Benz, G. Stark, E. Bamberg, P. C. Jordan, A. Fahr, and W. Brock. 1981. Relaxation studies of ion transport systems in lipid bilayer membranes. *Q. Rev. Biophys.* 14:513–598.

Liu, T. M., and D. Mauzerall. 1985. Distributed kinetics of decay of the photovoltage at the lipid bilayer-water interface. *Biophys. J.* 48:1–7.

Mauzerall, D., and C. M. Drain, 1992. Photogating of ionic currents across lipid bilayers: electrostatics of ions and dipoles inside the membrane. *Biophys. J.* 63:1544–1555.

Moore, W. J. 1962. Mobilities of hydrogen and hydroxy ions. *In* Physical Chemistry. 4th ed. Prentice-Hall, Englewood Cliffs, NJ. 338–340.

Pickar, H., and J. Hobbs. 1982. The influence of sterols on pentachlorophenol-induced charge transfer across lipid bilayers studied by alternating current methods. *Biochim. Biophys. Acta.* 693:221–236.

Schere, P. G., and J. Seelig. 1989. Electric charge effects on phospholipid head groups. Phosphatidylcholine in mixtures with cationic and anionic amphiphiles. *Biochemistry.* 28:7720–7728.

Seelig, J., and P. Ganz. 1991. Nonclassical hydrophobic effect in membrane binding equilibria. *Biochemistry.* 30:9354–9359.

Vanderkooi, J. M., and J. Callis. 1974. Pyrene. A probe of lateral diffusion in the hydrophobic region of membranes. *Biochemistry.* 13:4000–4006.

Vanderkooi, J., S. Fischkoff, B. Chance, and R. Cooper. 1974. Fluorescent probe analysis of the lipid architecture of natural and experimental cholesterol-rich membranes. *Biochemistry.* 13:1589–1595.

Woodle, M., and D. Mauzerall. 1986. Photoinitiated ion movements in bilayer membranes containing magnesium octaethylporphyrin. *Biophys. J.* 50:431–439.

Woodle, M., J. W. Zhang, and D. Mauzerall. 1987. Kinetics of charge transfer at the lipid bilayer-water interface on the nanosecond timescale. *Biophys. J.* 52:577–586.